EPJ Web of Conferences **40**, 15010 (2013)
DOI: 10.1051/epjconf/20134015010

$Pr_{0.5}Ca_{0.5}MnO_3$ thin films deposited on $LiNbO_3$ substrates

I. T. Gomes[1,2], B. G. Almeida[1], J. P. Araújo[2,3]

[1]Centro de Física, Universidade do Minho, Campus de Gualtar, 4710-057 Braga, Portugal
[2]IFIMUP/IN-Instituto de Nanociência e Nanotecnologia, R. Campo Alegre 4169-007 Porto, Portugal
[3]Universidade do Porto-DFA Faculdade de Ciências, R. Campo Alegre, 4169-007 Porto, Portugal

Abstract. Thin films of $Pr_{0.5}Ca_{0.5}MnO_3$ have been deposited on z-cut $LiNbO_3$ by pulsed laser ablation. The X-ray diffraction measurements showed that the films have grown highly oriented on $LiNbO_3$, with a pseudocubic (111) preferred growth direction. The thicknesses of the films, measured by low angle X-ray reflectivity, are between 13 and 140 nm. Their electrical resistivity present a semiconducting-like behaviour with an anomaly around 240 K, that corresponds to the charge ordering transition. The temperature of the transition (T_{CO}) was estimated from $ln\ \rho$ vs. $(1/T)$ plots. The charge ordering temperature was found to be dependent on the strain induced by the lattice mismatch on the films.

1 Introduction

The $Pr_{1-x}Ca_xMnO_3$ (PCMO) manganite exhibits a very broad composition range with charge and orbital ordering effects. A sufficiently strong static magnetic field applied to this system triggers an insulator to metal transition by which the charge- and orbital-ordered antiferromagnetic insulating ground state is melted into a conducting ferromagnetic metallic state, inducing colossal magnetoresistance [1-3]. The charge ordering transition is highly affected by pressure, electric and magnetic fields, radiation or stress. In particular, the strain induced in PCMO thin films by the lattice mismatch with the substrate may be able to modify its transport properties, namely the stabilization and modification of the charge-ordered phase [1-4]. Moreover, deposition of manganite thin films on piezoelectric substrates may allow for a tuneable control of these properties by applying an electric field to the substrate [5,6].

In this regard, lithium niobate ($LiNbO_3$) is ferroelectric up to 1210 °C and is commonly used in wave guide and integrated optics applications due to its optical, electro-optic, piezoelectric, photorefractive, elastic and photoelastic properties [7]. In the ferroelectric phase, $LiNbO_3$ possesses a trigonal structure, with R3c space group. The hexagonal lattice parameters are a_H = 5.145 Å and c = 13.86 Å [7].

Here, PCMO thin films have been deposited on z-cut lithium niobate crystalline substrates and their structural, magnetic and electrical properties were characterized. It is shown that the charge ordered phase is stabilized in PCMO thin films and that the corresponding transition temperature is correlated to the thickness of the manganite thin films.

2 Experimental

Thin films of $Pr_{0.5}Ca_{0.5}MnO_3$ (PCMO) were deposited by pulsed laser deposition using a KrF excimer laser (λ = 248 nm) at a fluence of 1.5 J/cm^2 and a 3 Hz repetition rate. The pulse duration was 20 ns and the target-to-substrate distance was 5.5 cm. During the deposition, the single-crystal substrates of z-cut $LiNbO_3$ were kept at 700 °C and the oxygen pressure was 0.8 mbar. Afterwards, the films were cooled down to room temperature at 10°C/minute under an atmospheric oxygen pressure.

For the laser ablation targets, polycrystalline samples of $Pr_{0.5}Ca_{0.5}MnO_3$ were prepared by the sol-gel combustion method. The obtained powder was then pressed into a pellet and underwent a series of annealings in order to increase its densification.

The X-ray diffraction (XRD) measurements were carried out in a Siemens D5000 diffractometer using Cu Kα radiation.

A standard four probe in-line technique with current inversion was used in the electrical resistance measurements. The current used in the measurements was 1 μA.

The temperature dependence of the magnetization was measured with a Quantum Design MPMS SQUID magnetometer, in the 5 – 350 K temperature range. First the samples were cooled to 5 K with zero applied field and the magnetization was measured with an applied field of 1300 Oe in the heating run (zero-field cooling, ZFC). Afterwards the sample was cooled with the same field,

and the field cooled measurement (FC) was carried out in the subsequent heating run.

3 Results and discussion

The thicknesses of the PCMO thin films were calculated from low-angle X-ray reflectivity (LAXRR) measurements. Figure 1 shows the reflectivity of a PCMO thin film, measured in the range $0.1° \leq 2\theta \leq 3°$.

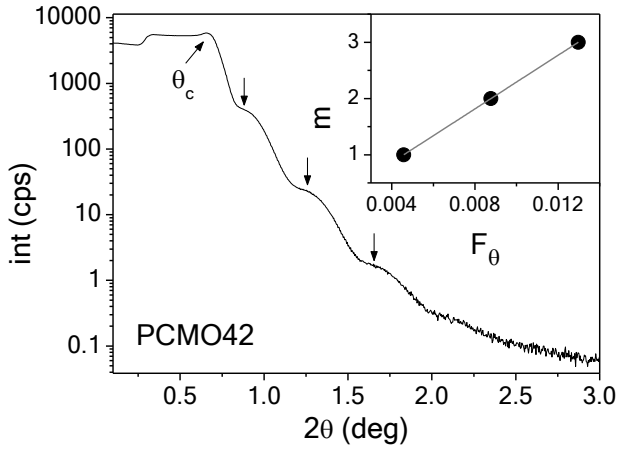

Fig. 1. LAXRR measurement of a PCMO thin film with a thickness of 18 nm. The vertical arrows mark the position of the Kiessig fringes, θ_m. The critical angle for total reflection θ_c is also marked. **Inset:** Kiessig fringes' order m as a function of F_θ. The grey line is the fit used to calculate the film thickness.

From the position of the Kiessig fringes (θ_m) and the value of the critical angle for total reflection (θ_c), the thickness (D) of the films was calculated using the equation [8]

$$m = \frac{1}{2} + \frac{2D}{\lambda}\sqrt{\cos^2\theta_C - \cos^2\theta_m}\,, \qquad (1)$$

where m is the order of the fringe. The thickness of the film is calculated from the slope of the linear fit to the plot of m as a function of $F_\theta = \sqrt{\cos^2\theta_C - \cos^2\theta_m}$, as shown in the inset of figure 1. The estimated thicknesses of the prepared samples were in the range 13 – 170 nm.

Figure 2 shows the X-ray diffractogram of a PCMO thin film with a thickness of 45 nm. The spectra were normalized to the intensity of the (006)-$LiNbO_3$ peak to compensate for the irradiated sample area and for better comparison. The trend on the normalized spectra is the same as on the original spectra. The peaks marked with an asterisk (*) belong to the substrate, while the remaining peaks belong to PCMO. The film is highly oriented, with a preferred pseudocubic (111) growth direction. There is also a small fraction of (110)-oriented grains, but the proportion between (110) and (111) does not change significantly with thickness.

Figure 3 shows an enlargement of the X-ray diffraction spectra on the 2θ region 38.5° - 42°, near the pseudocubic (111) PCMO peak, for all the samples. On the different films, this peak was fitted with a Gaussian function in order to determine peak positions and integral widths. The inset of figure 3 shows the obtained d_{111} out-of-plane interplanar distances, determined from the calculated peak positions using the Bragg equation. For the thinner film, the observed (111) peak is strongly deviated towards higher angles relative to bulk PCMO (vertical line on fig. 3). As such, its corresponding d_{111} out-of-plane interplanar distance is below the bulk d_{111} value, indicating a compressive strain along the growth direction. As the film thickness increases, this deviation generally decreases, so that the corresponding d_{111} progressively relaxes towards the bulk value, as shown in the inset of figure 3.

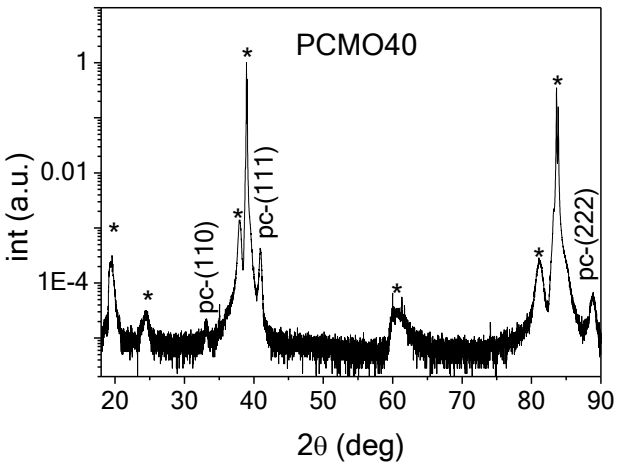

Fig. 2. X-ray diffraction spectrum of a PCMO thin film deposited on z-cut $LiNbO_3$ crystalline substrate, with a thickness D = 45 nm.

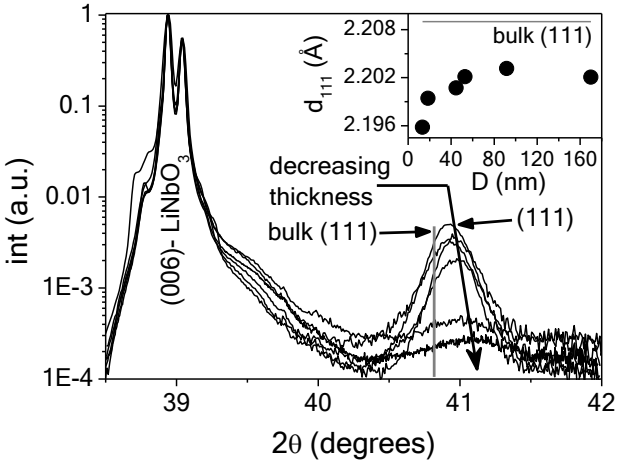

Fig. 3. PCMO pseudocubic (111) diffraction peak (the rightmost peak) of samples prepared with different thicknesses. The grey line marks the bulk diffraction peak position. **Inset:** Interplanar distance d_{111} as a function of film thickness. The grey line marks the bulk d_{111}.

The electrical resistance of the films was measured at low temperature, between 120 K and 300 K. The results of the resistance, normalized to its value at 300 K, are presented in figure 4. All the curves follow a semiconductor-like behaviour, where the electrical

resistance increases with decreasing temperature. The curves are similar for all samples near room temperature and below 150 K. However, for the intermediate temperature region 170 K ≤ T ≤ 290 K the curves differ from each other. On figure 4, the lower-lying curves belong to the thicker films.

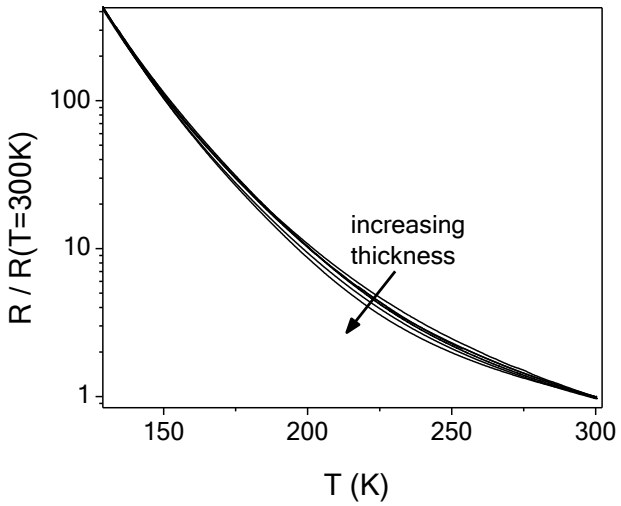

Fig. 4. Electrical resistance, normalized to its value at T = 300 K, of the PCMO thin film samples with different thicknesses. The arrow marks the trend with thickness.

The behaviour of the temperature dependence of the electrical resistivity resembles that of an activated process with $\rho = \rho_0 e^{E_a / k_B T}$, where ρ_0 is a constant and E_a is the activation energy. Hence, if the logarithm of the resistivity ρ was plotted as a function of the reciprocal temperature ($1/T$), a straight line should be obtained. However, as shown in figure 5, three regimes were obtained in the plot of ln ρ *vs.* ($1/T$), illustrated by the three different slopes observed on the experimental curve. In the high temperature region, the activation energy calculated from the slope of the linear fit is $E_a / k_B \approx$ 1200 K for all films, which is consistent with the formation of small polarons [4,9].

As the temperature approaches 240 K, a change of slope is observed in the curves. This is attributed to the onset of the charge ordering transition on the films [2,4]. Further evidence for the presence of a charge ordering transition is given by the temperature dependence of the magnetization (see inset of figure 5). Both the zero-field-cooled (ZFC) and field-cooled (FC) measurements present a maximum in the magnetization around 240 K, which is more evident in the thicker films.

In order to obtain the charge-ordering transition temperature (T_{CO}), the temperature of the intersection of the linear fits to the high and intermediate temperature ranges, in the ln ρ *vs.* ($1/T$) plot, was determined, as exemplified in figure 5, and its value was attributed to T_{CO}.

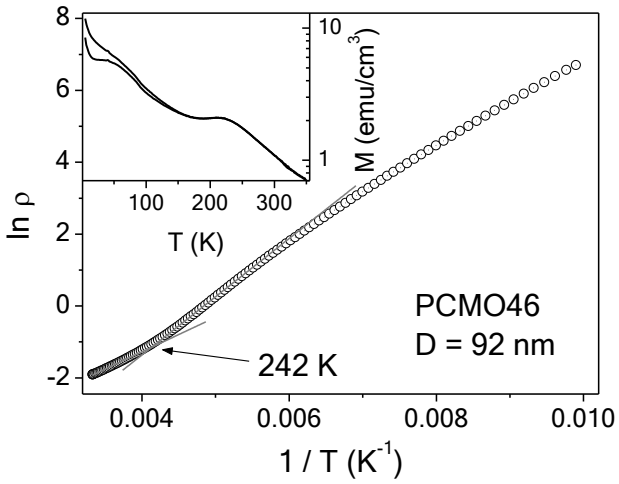

Fig. 5. Plot of ln ρ *vs.* ($1/T$) and corresponding linear fits for the calculation of T_{CO}. **Inset:** Temperature dependence of the magnetization for the same PCMO film.

Figure 6 shows the obtained charge ordering transition temperatures plotted as a function of the corresponding film thicknesses. It is found that its value decreases as the thickness of the films increases.

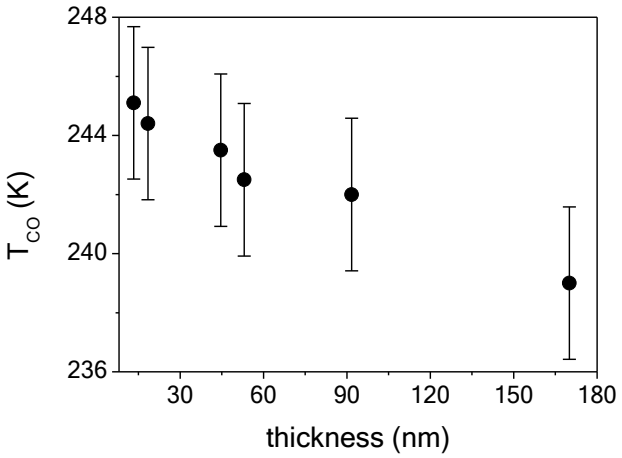

Fig. 6. Film-thickness dependence of the charge ordering transition temperature of the PCMO thin films.

Since the films are highly textured along the (111) direction, the (110) residual phase is similar on all samples and since the normalized resistance of all films is roughly equal in the low and high temperature regions, the influence of extrinsic factors in the transport properties, such as grain boundaries and poor crystallinity, may be ruled out. However, the influence of the strain due to lattice mismatch with the substrate, as observed on the XRD results of figure 3, cannot be ruled out, particularly on the thinner films.

The strain along the pseudocubic (111)-PCMO thin films growth direction, $\varepsilon = \left(d_{111}^{film} - d_{111}^{bulk} \right) \Big/ d_{111}^{bulk} \times 100\%$, was calculated. Figure 7 shows the charge ordering temperature as a function of the calculated strain on the

films. A systematic increase of T_{CO} with increasing compressive strain is observed for the thinner films, indicating a progressive stabilization of the charge ordering phase with increasing strains.

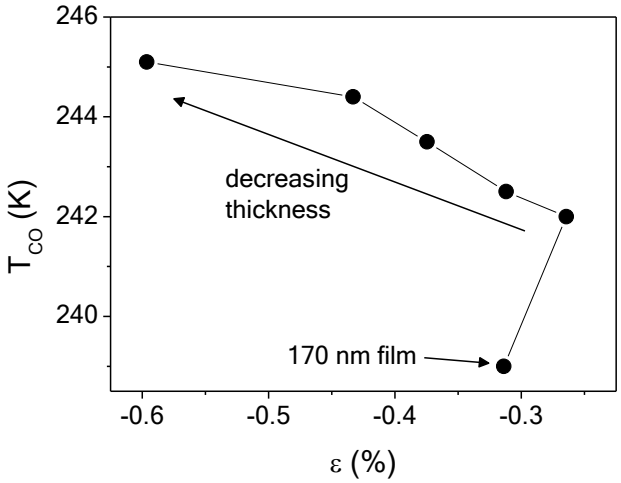

Fig. 7. Dependence of the charge ordering transition temperature on the out-of-plane strain in the PCMO thin films.

In fact, the enhancement of the charge ordering temperature with decreasing thickness has been observed in PCMO thin films deposited on $SrTiO_3$ crystal substrates [4]. This effect was attributed to the presence epitaxial strains that promoted the stabilization of the charge ordered phase for thinner films. Therefore, here, the observed systematic decreasing of T_{CO} with the PCMO film thickness can be attributed to the progressive relaxation of substrate induced strains as the films thickness is increased.

4 Conclusion

PCMO thin films were deposited on z-cut $LiNbO_3$ crystal substrates with different thicknesses and their structural, magnetic and electrical properties were characterized. The films were highly oriented, with a pseudocubic (111) preferential growth direction. The charge-ordered phase was observed to be stabilized even in the thinner films and the corresponding transition temperature was found to depend on film thickness. This correlation was attributed to the strain imposed by the substrate onto the films, which is stronger in the thinner samples and progressively relaxes with increasing thickness of the films.

References

1. W. Prellier, E.R. Buzin, Ch. Simon, B. Mercey, M. Hervieu, S. de Brion and G. Chouteau, Phys. Rev B **66,** 024432 (2002)
2. Y.Q. Zhang, Y.L. Zhu Z.D. Zhang and J. Aarts, J. Appl. Phys. **101,** 063919 (2007)
3. Y. Z. Chen, J. R. Sun, S. Liang, W. M. Lv, B. G. Shen and W. B. Wu, J. Appl. Phys. **103**, 096105 (2008)
4. Z.Q. Yang, Y.Q. Zhang, J. Aarts, M.-Y. Wu and H.W. Zandbergen, Appl. Phys. Lett. **88**, 072507 (2006)
5. K. Dörr, C. Thiele, J.-W. Kim, O. Bilani, K. Nenkov and L. Schultz, Phil. Mag. Lett. **87**, 269 (2007)
6. R. K. Zheng, C. Chao, H. L. W. Chan, C. L. Choy, and H. S. Luo, Phys. Rev. B **75**, 024110 (2007)
7. R.S. Weis and T.K. Gaylord, Appl. Phys. A **37**, 191 (1985)
8. I.T. Gomes, B.G. Almeida, A.M.L. Lopes, J.P. Araújo, J. Barbosa and J. Mendes, J. Magn. Magn. Mater. **322**, 1174 (2010)
9. Palstra, T. T. M.; Ramirez, A. P.; Cheong, S.-W.; Zegarski, B. R.; Schiffer, P.; Zaanen, J., Phys. Rev. B **56**, 5104 (1997)